 ISSN 0267-8179. DOI: 10.1002/jqs.1552

Late Quaternary tephrostratigraphy, Ahklun Mountains, SW Alaska

DARRELL S. KAUFMAN,[1]* BRITTA J. L. JENSEN,[2] ALBERTO V. REYES,[2]† CALEB J. SCHIFF,[1] DUANE G. FROESE[2] and NICHOLAS J. G. PEARCE[3]

[1]School of Earth Sciences and Environmental Sustainability, Northern Arizona University, Flagstaff, AZ 86011-4099, USA
[2]Department of Earth and Atmospheric Sciences, University of Alberta, Edmonton, Alberta, Canada
[3]Institute of Geography & Earth Sciences, Aberystwyth University, Aberystwyth, UK

Received 24 April 2011; Revised 21 September 2011; Accepted 29 September 2011

ABSTRACT: Radiocarbon-dated sediment cores from six lakes in the Ahklun Mountains, south-western Alaska, were used to interpolate the ages of late Quaternary tephra beds ranging in age from 25.4 to 0.4 ka. The lakes are located downwind of the Aleutian Arc and Alaska Peninsula volcanoes in the northern Bristol Bay area between 159° and 161°W at around 60°N. Sedimentation-rate age models for each lake were based on a published spline-fit procedure that uses Monte Carlo simulation to determine age model uncertainty. In all, 62 ^{14}C ages were used to construct the six age models, including 23 ages presented here for the first time. The age model from Lone Spruce Pond is based on 18 ages, and is currently the best-resolved Holocene age model available from the region, with an average 2σ age uncertainty of about $\pm$ 109 years over the past 14.5 ka. The sedimentary sequence from Lone Spruce Pond contains seven tephra beds, more than previously found in any other lake in the area. Of the 26 radiocarbon-dated tephra beds at the six lakes and from a soil pit, seven are correlated between two or more sites based on their ages. The major-element geochemistry of glass shards from most of these tephra beds supports the age-based correlations. The remaining tephra beds appear to be present at only one site based on their unique geochemistry or age. The 5.8 ka tephra is similar to the widespread Aniakchak tephra [3.7 $\pm$ 0.2 (1σ) ka], but can be distinguished conclusively based on its trace-element geochemistry. The 3.1 and 0.4 ka tephras have glass major- and trace-element geochemical compositions indistinguishable from prominent Aniakchak tephra, and might represent redeposited beds. Only two tephra beds are found in all lakes: the Aniakchak tephra (3.7 $\pm$ 0.2 ka) and Tephra B (6.1 $\pm$ 0.3 ka). The tephra beds can be used as chronostratigraphic markers for other sedimentary sequences in the region, including cores from Cascade and Sunday lakes, which were previously undated and were analyzed in this study to correlate with the new regional tephrostratigraphy.

KEYWORDS: tephra; tephrochronology; Quaternary stratigraphy; Aleutian arc; Alaska Peninsula.

Introduction

Tephra deposits are key stratigraphic markers. They can be readily characterized geochemically, and are deposited essentially instantaneously across the landscape. Once the tephrostratigraphy has been developed for a region, tephra beds can be used for precise correlations among ice, marine, lacustrine and terrestrial depositional environments (Lowe, 2011 provides a recent review of tephrochronology, including tephrostratigraphy and its applications).

The Ahklun Mountains in the Bristol Bay region of south-western Alaska are located downwind of the Aleutian Arc and western Alaska Peninsula, where they have received tephra fall from explosive volcanism throughout the Quaternary. At least eight Holocene caldera-forming eruptions with bulk volumes >10 km^3 have occurred within 1000 km of the Ahklun Mountains (Miller and Smith, 1987). Despite the frequency of large, relatively proximal eruptions, however, few regional tephra deposits have been described in the region. Previous work on coastal bluffs around Bristol Bay revealed multiple Quaternary tephra deposits interbedded with loess, peat and glacial–marine sediment (Kaufman *et al.*, 2001). The most prevalent and thickest of these is the Aniakchak tephra, which forms a widespread mid-Holocene marker across western Alaska (Riehle *et al.*, 1987; Begét *et al.*, 1992).

The Ahklun Mountains has an unusually high concentration of topographically closed basins that contain lakes. The range was extensively eroded by repeated advances of Pleistocene glaciers, which carved over-deepened troughs and deposited extensive hummocky drift (Manley *et al.*, 2001). Tephra are well preserved in the sediments of lakes in the Ahklun Mountains, where they can be recovered by standard lake-coring procedures and dated using radiocarbon analysis of associated macrofossils. Indeed, sediments from all of the lakes that we have cored in the Ahklun Mountains contain multiple tephra layers. The longest lake cores recovered to date are from Arolik Lake, where Kaufman *et al.* (2003) reported six visually prominent tephra layers deposited since about 24 ka. Additional cryptotephra are probably also present, but have not been investigated.

During the past 15 years, multiple lakes have been cored from across the Ahklun Mountains, primarily to recover sedimentary records of past environmental change. The purpose of this study is to develop the late Quaternary tephrostratigraphy for the Ahklun Mountains by determining accurate ages for visually prominent tephra beds that are characterized by glass major-element geochemistry. This tephrostratigraphy will be useful for age control and for high-precision correlations in future studies of Quaternary records from the region.

Methods

Tephra selected for this study

This study documents the visually prominent tephra deposits in radiocarbon-dated sediment cores from six lakes located across the Ahklun Mountains (Table 1). Tephra deposits from two other lakes without other age control are also analyzed. The lakes are separated by up to 125 km, from Arolik Lake in the west to Lone Spruce Pond in the east (Fig. 1). Except for Lone Spruce Pond (informal name), background information on all of

*Correspondence: D. S. Kaufman, as above.
E-mail: darrell.kaufman@nau.edu
† Present address: Department of Geoscience, University of Wisconsin-Madison, Madison, Wisconsin, USA.

Table 1. Location and other information about the study lakes and their sediment.

Lake	Latitude (°N)	Longitude (°W)	Elevation (m)	Maximum depth (m)	Lake area (km^2)	Average accumulation rate (mm a^{-1})*	Number of ages per 1000 a	Average uncertainty (a)†
Arolik Lake[a]	59.47	161.12	145	53	2.0	0.23	0.52	316
Cascade Lake[b]	60.14	159.4	335	55	3.1	Not dated	—	—
Little Swift[c]	60.21	159.76	572	24	0.7	0.46	0.71	221
Lone Spruce[d]	60.01	159.14	112	22	0.2	0.25	1.48	109
Nimgun[e]	59.56	160.77	320	8	0.4	0.28	0.80	155
Sunday Lake[f]	59.67	159.47	173	13	0.5	Not dated	—	—
Sunday Pond[g]	59.67	159.45	177	6	0.1	0.36	1.47	112
Waskey[h]	59.88	159.21	150	8	0.2	0.45	0.72	201

* Excludes tephra beds. † One-half of the 2σ range output by *clam* (Blaaw, 2010) evaluated at 1-cm intervals over dated range. References: [a] Kaufman *et al.* (2003), [b] Kathan (2006), [c] Axford and Kaufman (2004), [d] This study, [e] Hu *et al.* (2002) and this study, [f] Feinberg (2000), [g] Feinberg (2000) and this study, [h] Levy *et al.* (2004).

the lakes has been reported previously, including specific coring procedures, geomorphological setting and bathymetry, and the lithostratigraphy of their sediments (Table 1). The tephra were distinguished from the ambient lacustrine sediment by their (i) contrasting color, (ii) higher magnetic susceptibility (MS) value, (iii) coarser grain size and (iv) lower organic-matter content. Grains from layers identified by these criteria were examined using light and scanning electron microscopy (SEM) to confirm the presence of volcanic glass.

Determining tephra ages

Sediment cores were sampled for plant macrofossils, which were submitted to several laboratories for accelerator mass spectrometry (AMS) ^{14}C analysis (Table 2). All ages were calibrated to calendar years using IntCal09 (Reimer *et al.*, 2009) and *calib* (v 5.0.2; Stuiver and Reimer, 1993). Unless indicated otherwise, all ^{14}C ages in the text are reported as calendar years prior to 1950 AD (cal a BP). Age models were constructed by fitting the age–depth data with a smoothed spline using the *clam* code (Blaauw, 2010) for the open-source statistical software 'R' (R Development Core Team, 2010). The routine generates Monte Carlo age–depth fits through the calibrated-age probability distributions; it then calculates the best-fit age–depth curve as the weighted average of 10 000 iterations. The confidence intervals are calculated as the 2σ range of the mean of the iterations. The default level of smoothing for the spline fit (0.3) was used because it was flexible enough to intersect the 2σ calibrated age range of nearly all ^{14}C ages. In general, more flexure would have generated unrealistically rapid sedimentation-rate changes without corresponding changes in sediment lithology, and more smoothing would have bypassed ^{14}C ages that could not otherwise be rejected. The core depth for each ^{14}C sample was adjusted by subtracting the cumulative thickness of the overlaying tephra layers, which were assumed to have been deposited instantly. Modeled tephra ages and associated uncertainties were taken from the 1-cm-interval output of the *clam* routine.

For $^{239+240}Pu$ analyses, the top 20 cm of the surface core from Lone Spruce Pond was sampled at 0.5-cm intervals and dry-ashed at 550°C. Samples were spiked with 10 pg of ^{242}Pu tracer, leached overnight at 80°C with 5 mL of 16 M HNO_3, and Pu was separated using TEVA resin (EIChrom, Darien, IL, USA). Additional details of the chemical procedures are given in Ketterer *et al.* (2004). Pu was measured with a Therm X Series II quadrupole ICP-MS equipped with an APEX HF high-efficiency sample introduction system (ESI Scientific, Omaha, NE, USA).

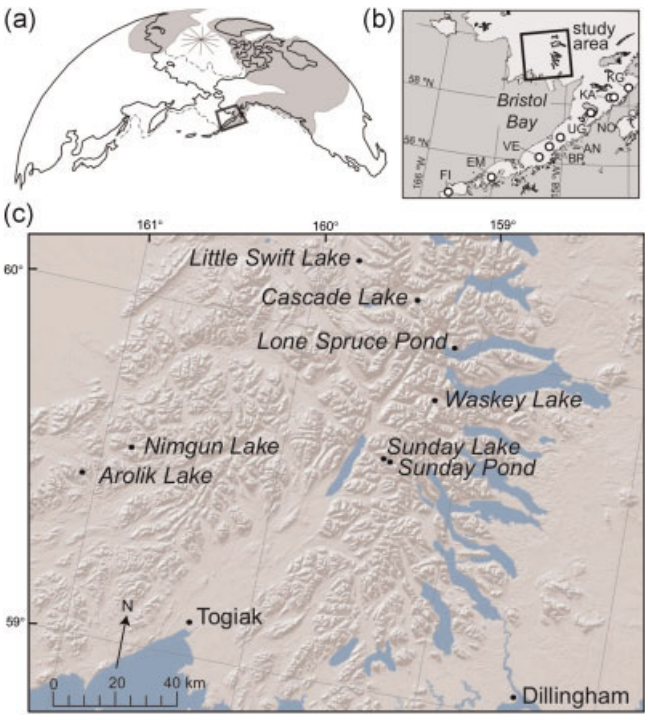

Figure 1. (a) Location of the Bristol Bay region relative to (b) major Holocene calderas, with a map of (c) the Ahklun Mountains showing the location of eight lakes included in this study. Gray shading in (a) is the approximate extent of glacier ice during the last glacial maximum. Calderas in (b) are: FI, Fisher; EM, Emmons Lake; VE, Veniaminof; BP, Black Peak; AN, Aniakchak; UG, Ugashik-Peulik; KA, Katmai; NO, Novarupta; KG, Kaguyak. This figure is available in colour online at wileyonlinelibrary.com.

Tephra geochemistry

Glass major-element geochemistry was analyzed on a JEOL 8900 electron microprobe at the University of Alberta, using wavelength-dispersive spectrometry. A reduced beam current of 6 nA and defocused beam of 10 μm diameter was used to minimize alkali loss during analyses; accelerating voltage was set at 15 keV. Two secondary standards, a Lipari obsidian and Old Crow tephra, were analyzed concurrently with the unknown samples. Potential correlatives were identified and re-analyzed concurrently to minimize minor differences that can occur between different analytical runs. We used backscatter electron imaging to minimize analysis of glass shards with substantial microcrystalline contamination.

Table 2. Radiocarbon and surface ages used to develop the age models.

Core	Midpoint depth (cm)		Sample thickness (cm)	AMS Lab ID	Lab. no.	^{14}C age (a BP)	Calibrated age* (a BP)	Material†	Ref.‡	Rej.§
	Tube	Tephra-free								
Arolik Lake										
AL-4	4.0	4.0	2.0	NRSL	11363	2390 ± 65	2456 ± 168	Mixed macrofossils	1	
AL-4	11.0	11.0	0.0	NRSL	11364	2590 ± 85	2653 ± 145	Wood	1	
AL-4	65.0	65.0	2.0	NRSL	11365	2800 ± 45	2904 ± 54	Wood	1	1
AL-4	111.5	83.5	1.0	CAMS	86531	5295 ± 30	6082 ± 90	Leaves; other macros	1	
AL-4	137.0	109.0	2.0	NRSL	11366	6150 ± 55	7054 ± 85	Mixed macrofossils	1	
AL-4	158.5	129.0	1.0	CAMS	86532	7515 ± 35	8350 ± 29	Moss	1	
AL-4	182.0	154.0	0.0	NRSL	11367	9310 ± 65	10508 ± 119	Wood	1	
AL-4	200.5	172.5	1.0	CAMS	86533	8905 ± 35	10036 ± 115	Wood	1	
AL-4	247.0	219.0	2.0	NRSL	11368	9960 ± 95	11461 ± 176	Mixed macrofossils	1	
AL-4	254.0	225.0	2.0	CAMS	79689	10550 ± 230	12357 ± 323	Wood (small sample)	1	
AL-4	277.5	248.5	1.0	CAMS	79689	11850 ± 40	13709 ± 47	Single twig	1	
AL-4	320.0	291.0	2.0	NRSL	11369	10970 ± 75	12843 ± 52	Mixed macrofossils	1	1
AL-4	331.5	294.5	3.0	CAMS	81525	7160 ± 210	7989 ± 114	Moss (small sample)	1	1
AL-4	362.5	325.5	1.0	CAMS	81526	13875 ± 50	16947 ± 201	Large wood	1	
AL-4	363.0	326.0	2.0	CAMS	81527	13650 ± 110	16788 ± 231	Moss	1	
AL-4	367.0	330.0	2.0	NRSL	11544	9880 ± 55	11286 ± 33	Mixed macrofossils	1	1
AL-4	392.5	355.5	1.0	CAMS	81528	12490 ± 80	15506 ± 236	Mixed macrofossils	1	1
AL-4	423.0	386.0	2.0	NRSL	11545	13190 ± 65	16082 ± 183	Mixed macrofossils	1	1
AL-4	481.0	443.0	2.0	NRSL	11546	15890 ± 75	19106 ± 89	Mixed macrofossils	1	
AL-4	692.0	654.0	2.0	NRSL	11370	20530 ± 130	24511 ± 219	Mixed macrofossils	1	
AL-4	747.0	708.0	4.0	NRSL	11547	24800 ± 140	29652 ± 22	Mixed macrofossils	1	
AL-4	799.0	760.0	2.0	NRSL	11371	28500 ± 220	32866 ± 372	Mixed macrofossils	1	
AL-4	850.0	811.0	2.0	NRSL	11372	30730 ± 260	35210 ± 651	Mixed macrofossils	1	
Little Swift Lake										
LS-A	22.5	22.5	5.0	NRSL	11065	1600 ± 40	1478 ± 58	Wood	2	
LS-A	22.5	22.5	5.0	NRSL	11066	1660 ± 40	1564 ± 80	Mixed macrofossils	2	
LS-A	124.5	124.5	3.0	NRSL	11067	2810 ± 40	2913 ± 48	Mixed macrofossils	2	
LS-A	204.5	204.5	5.0	NRSL	11068	3840 ± 40	4254 ± 111	Mixed macrofossils	2	
LS-A	340.5	316.5	5.0	NRSL	11069	6230 ± 45	7153 ± 110	Mixed macrofossils	2	
LS-A	405.0	380.8	4.0	NRSL	11070	7550 ± 75	8359 ± 103	Mixed macrofossils	2	
LS-A	449.5	424.5	5.0	NRSL	11071	9390 ± 55	10621 ± 67	Mixed macrofossils	2	
LS-A	510.5	480.0	5.0	CAMS	76366	10640 ± 170	12718 ± 281	Mixed macrofossils	2	1
LS-A	547.5	522.5	5.0	NRSL	11059	11200 ± 75	13101 ± 101	Mixed macrofossils	2	1
LS-A	569.5	544.5	3.0	NRSL	11060	10760 ± 75	12801 ± 51	Mixed macrofossils	2	
Lone Spruce Pond										
09-LSP-4A	0.8	0.8	0.5	—	—	—	−3 ± 10	Pu onset (no peak in core)	3	
07-LSP-3	0.8	23.8	0.5	UCIAMS	37816	200 ± 15	168 ± 144	Leaf fragments	3	
09-LSP-4A	35.1	34.9	0.2	UCIAMS	72311	360 ± 60	406 ± 86	Terrestrial leaf fragments; moss stems and leaves	3	
07-LSP-3	23.3	46.1	0.5	UCIAMS	37817	595 ± 15	607 ± 41	Leaf fragments	3	
09-LSP-4A	53.5	53.3	1.0	CAMS	144702	570 ± 170	566 ± 180	Unidentified	3	
07-LSP-3	46.8	69.6	0.5	UCIAMS	37818	1150 ± 15	1052 ± 36	Leaf fragments	3	
07-LSP-3	74.8	97.6	0.5	UCIAMS	37819	1600 ± 25	1471 ± 57	Leaf fragments	3	
07-LSP-3	120.3	143.1	0.5	UCIAMS	37820	2435 ± 35	2477 ± 158	Leaf fragments	3	
07-LSP-3	140.5	163.3	1.0	UCIAMS	37821	2875 ± 15	2995 ± 51	Leaf fragments	3	
07-LSP-3	186.5	184.2	1.0	UCIAMS	37822	3575 ± 20	3875 ± 25	Leaf fragments	3	
07-LSP-3	206.3	204.0	0.5	UCIAMS	37823	3905 ± 15	4356 ± 58	Leaf fragments	3	
07-LSP-3	219.5	217.2	1.0	UCIAMS	37824	4090 ± 15	4575 ± 126	Leaf fragments	3	
07-LSP-3	280.5	261.0	1.0	UCIAMS	72311	5320 ± 15	6080 ± 81	Woody fragments; moss stems and leaves	3	
07-LSP-3	283.5	264.0	1.0	UCIAMS	37825	5330 ± 15	6103 ± 80	Leaf fragments	3	
07-LSP-3	320.5	301.0	1.0	UCIAMS	37826	7075 ± 15	7893 ± 34	Unidentified	3	
07-LSP-3	333.5	314.0	1.0	UCIAMS	83790	8910 ± 120	9989 ± 39	*Daphnia* egg case, *Juncus* seed, Bryophyte, Bryozoan	3	
07-LSP-3	340.0	320.5	2.0	UCIAMS	82294	11610 ± 35	13440 ± 71	Moss, chitin, terrestrial leaf, woody fragments	3	2
07-LSP-3	344.5	325.0	1.0	UCIAMS	83791	11120 ± 70	13002 ± 98	*Daphnia*, Bryozoa, isoetes spore, chitin	3	2
07-LSP-3	356.5	337.0	1.0	UCIAMS	83792	10620 ± 30	12584 ± 29	Bryophyte stems, unidentified vegetation	3	
07-LSP-3	360.0	340.5	2.0	UCIAMS	82295	10330 ± 60	12176 ± 167	Aquatic moss, chitin	3	
07-LSP-3	379.0	358.5	2.0	CAMS	144698	17740 ± 2680	21271 ± 3224	Unidentified	3	

(*Continues*)

Table 2 (Continued)

Core	Midpoint depth (cm)		Sample thickness (cm)	AMS Lab ID	Lab. no.	^{14}C age (a BP)	Calibrated age* (a BP)	Material†	Ref.‡	Rej.§
	Tube	Tephra-free								
07-LSP-3	379.5	359.0	1.0	UCIAMS	72309	21260 ± 2100	25431 ± 2522	Woody fragments; moss stems	3	
07-LSP-3	400.0	380.1	2.0	CAMS	144828	20440 ± 80	24385 ± 141	Bulk sediment	3	
Nimgun Lake										
NL-2	159.0	91.0	1.0	NRSL	10554	3650 ± 40	3971 ± 85	Macro from within tephra (adjusted to 206 cm depth)	3	
NL-2	228.0	113.0	2.0	NRSL	11549	4360 ± 35	4925 ± 48	Twig	3	
NL-2	296.0	179.0	1.0	NRSL	10556	7640 ± 100	8447 ± 212	Mixed macrofossils	3	2
NL-2	344.0	226.0	0.0	NRSL	10557	7620 ± 50	8418 ± 38	Wood	4	
NL-2	379.0	261.0	0.0	AA	26594	9030 ± 85	10187 ± 165	Mixed macrofossils	4	
NL-2	401.0	283.0	0.0	CAMS	73100	9370 ± 50	10597 ± 71	Twig	4	
NL-2	407.0	289.0	2.0	CAMS	76365	9380 ± 110	10613 ± 170	Mixed plant	4	
NL-2	421.0	303.0	2.0	NRSL	11551	10500 ± 80	12508 ± 118	Grass & seeds	4	1
NL-2	466.0	347.0	2.0	NRSL	11552	11070 ± 60	12992 ± 61	Twig & moss	4	
NL-2	494.0	375.0	2.0	AA	26593¶	12110 ± 85	13964 ± 98	Grass & moss	4	
Sunday Pond										
SP-1	328.0	182.0	0.5	NSRL	12336	3630 ± 85	3951 ± 122	Wood	3	
SP-1	340.5	194.5	1.0	UCIAMS	72360	3700 ± 50	4040 ± 85	Terrestrial leaf fragments; stem fragments	3	
SP-1	364.5	218.5	1.0	UCIAMS	72361	4140 ± 35	4684 ± 115	Unidentified plant fragments	3	
SP-1	410.5	262.5	1.0	NSRL	12337	5980 ± 40	6819 ± 65	Wood	3	
SP-1	427.5	277.5	1.0	UCIAMS	72362	6410 ± 60	7343 ± 63	Terrestrial leaf fragments (?); bud	3	
Waskey Lake										
WL-1	0.0	0.0	0.0	—	—	—	−50 ± 1	Extrapolated surface	5	
WL-1	18.0	23.0	4.0	NSRL	11769	170 ± 35	176 ± 143	Mixed macrofossils	5	
WL-1	89.0	94.0	2.0	NSRL	11770	550 ± 40	562 ± 51	Vegetation	5	
WL-1	194.0	199.0	2.0	NSRL	11771	2700 ± 35	2802 ± 42	Vegetation	5	
WL-1	281.0	286.0	2.0	NSRL	11772	3140 ± 35	3370 ± 50	Vegetation	5	
WL-1	479.0	334.0	2.0	NSRL	11773	4450 ± 60	5093 ± 155	Vegetation	5	
WL-1	588.5	430.5	3.0	NSRL	11774	8120 ± 70	9071 ± 125	Mixed macrofossils	5	
WL-1	650.5	503.5	1.0	NSRL	11058	9710 ± 90	11092 ± 201	Mixed macrofossils	5	
WL-2	34.0	34.0	2.0	NSRL	11553	160 ± 35	172 ± 184	Mixed macrofossils	3	3
Soil pit near Cascade Lake										
—	6	—	1.0	UCIAMS	23856	435 ± 15	505 ± 20	Wood & leaves		

* Median probability age (Telford *et al.*, 2004) ± one-half of the 2-sigma calibrated age range. † Mixed macrofossils = various proportions of mosses, sedges, seeds, leaves, wood fragments and insects. ‡ Ref: 1 = Kaufman *et al.* (2003), 2 = Axford and Kaufman (2004), 3 = this study; 4 = Hu *et al.* (2002), 5 = Levy *et al.* (2004). § Rej: 1 = rejected, see orignal reference; 2 = rejected, this study; 3 = from second core not used in age model. ¶ Lab. number listed incorrectly in original reference.

Individual glass shards were analyzed with a minimum goal of at least 20 analyses per sample. This number was occasionally unattainable for glass-poor samples with fine-grained or detrital shards. Analyses with totals less than ~94% were discarded. The major-element geochemistry of each sample was examined through bivariate plots to identify coherent geochemical populations and eliminate outliers. Outliers were defined as analyses with oxide values beyond the 2σ (3σ for wt% NaO) average of the main geochemical population(s) or trend. Outliers probably result from the accidental analysis of mineral microcrysts within the glass shards, or of detrital glass, which do not conform to the petrologically consistent geochemical trend of a sample.

Trace-element analyses were conducted on a subset of 'Aniakchak-like' tephra samples (UA 1963, 1964, 1974, 1976, 1783) that could not be distinguished by their major-element geochemistry (discussed below). These samples were analyzed by laser ablation inductively coupled plasma mass spectrometry (LA-ICP-MS) using a Coherent GeoLas ArF 193-nm Excimer laser ablation system coupled to the Thermo Finnegan Element 2 sector field ICP-MS at the University of Aberystwyth. Analyses were performed on individual shards using 20- and 14-μm-diameter ablation craters at a laser energy of 10 J cm^2 at a repetition rate of 5 Hz with a 24-s acquisition time. ^{29}Si was used as the internal standard, with average compositions determined from electron microprobe analyses, and normalized to an anhydrous basis. For samples with bi-modal major-element composition (i.e. rhyolitic and andesitic populations), the low Ca/Si ratio was assigned to the rhyolitic population and the high ratio to the andesitic population. Calibration was achieved against the NIST SRM 612 using the concentrations given in Pearce *et al.* (1997). Further details of the analytical methodologies, precision and accuracy are given in Pearce *et al.* (2011). The MPI-DING reference rhyolitic glass ATHO-G was analyzed as a monitor of the method (Jochum *et al.*, 2006).

Results

Age models

Sixty-two AMS ^{14}C ages distributed among the six lakes were used to develop the age models (Fig. 2). Of these ages, 23 are published here for the first time. An additional 15 ages were rejected for reasons discussed by the original authors, and are

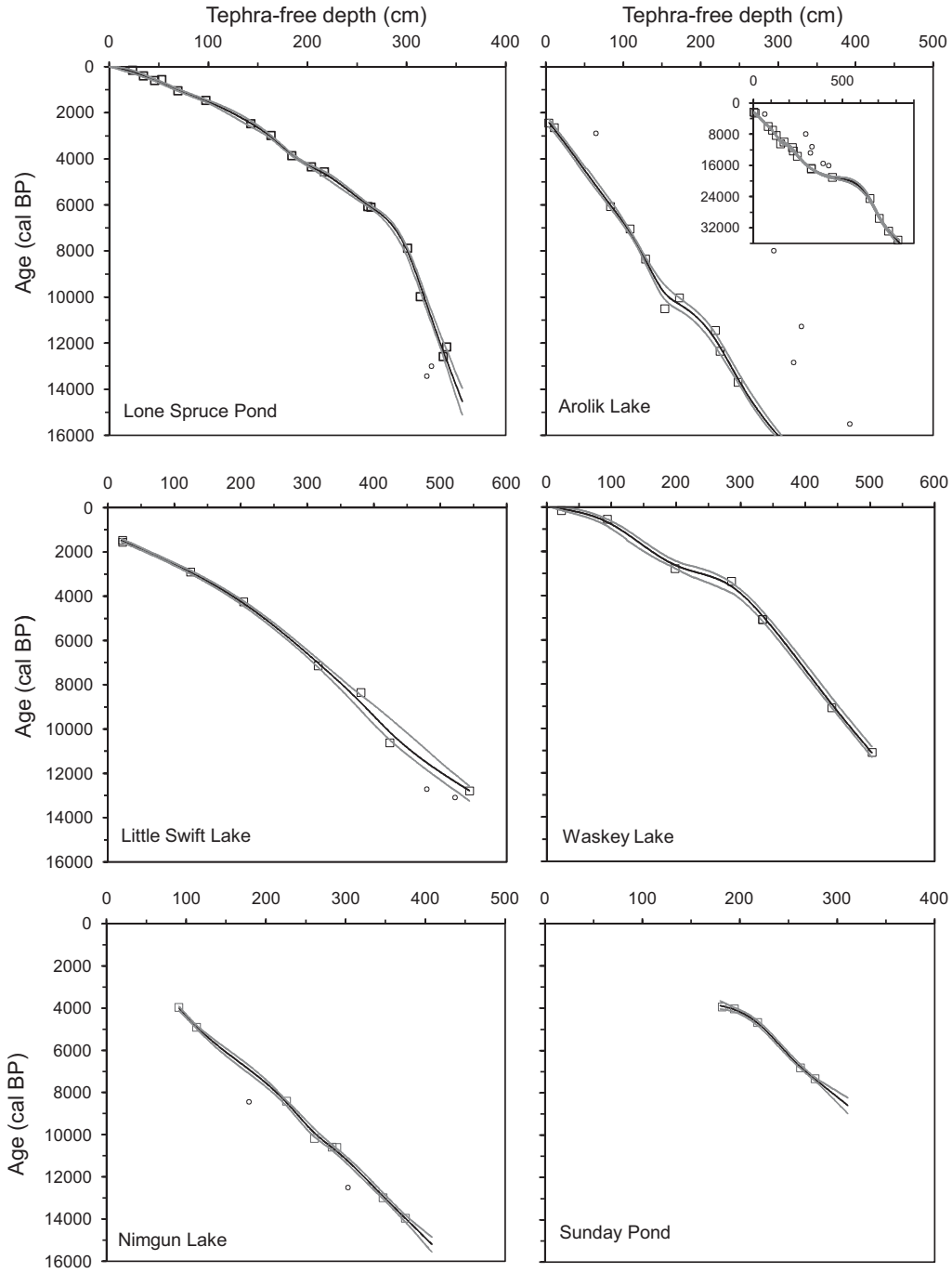

Figure 2. Age–depth models for sediment cores from each of the six lakes included in this study. The squares show median values of the calibrated-age probability density functions of ^{14}C ages (Telford *et al.*, 2004) as output by *calib* (Stuiver and Reimer, 1993). The 1σ calibrated age range falls within the size of the symbol for nearly all ages. Open circles are ages rejected by the original authors. Gray lines are 95% confidence intervals as output by the age–depth modeling routine *clam* (Blaauw, 2010). Curves are extrapolated beyond the ^{14}C age control only where they are used to infer the ages of tephra beds. All *y*-axis scales are equivalent (0–16 ka); inset: the full age–depth relation for the longest core, which is from Arolik Lake. The full data are given in Table 2.

listed in Table 2. The age–depth models generated in this study provide a consistent treatment among the study lakes; they supersede the slightly different age–depth models that were published previously, which were based on polynomial or other regression fits. On the basis of the confidence intervals evaluated at 1-cm intervals, the uncertainty (one-half of the 2σ range) in the age models ranged from ± 109 a for Lone Spruce Pond, with the most ages (1.48 per 1000 years), to ± 316 a for Arolik Lake, with the fewest ages (0.52 per 1000 years) (Table 1). The average sedimentation rate for the six lakes based on the age models is 0.34 mm a^{-1}. More specific information about the sediment cores and their age models is summarized below, with the lakes presented from east to west.

Lone Spruce Pond

Lone Spruce Pond (informal name) is located in the north-eastern Ahklun Mountains (Fig. 1). A 4.7-m-long composite core (LSP-3/4) was recovered from the depocenter at 22 m water depth, and has not been described previously. It contains the best-dated stratigraphic sequence obtained to date from the Ahklun Mountains, extending to about 14.5 ka and including seven visually obvious tephra layers, more than any other lake cored in the region. The sedimentary sequence serves as a reference for the regional tephrostratigraphy (Fig. 3). The sediment has been analyzed for multiple paleoenvironmental proxies, which will be presented in a subsequent study, along

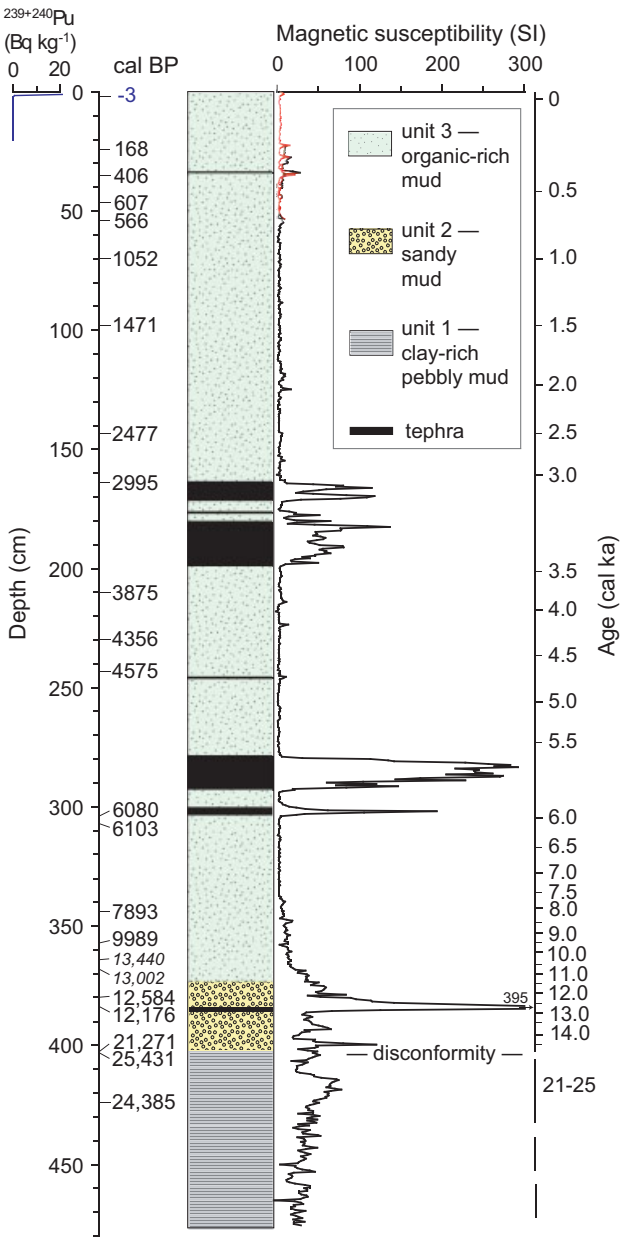

Figure 3. Lone Spruce Pond stratigraphic sequence with $^{239+240}$Pu profile, ^{14}C ages (Table 2) and magnetic susceptibility (MS) profile (07-LS-3). Red MS profile is from the surface core (09-LS-4A). The age–depth model (Fig. 2) was used for the right-hand scale. This core contains more tephra beds over the last 14.5 ka than any other from the region. This figure is available in colour online at wileyonlinelibrary.com.

with further details about the pond and its sedimentary sequence.

Briefly, core LSP-3/4 comprises three major lithologic units (Fig. 3). Unit 1 (477–399 cm; ~25–22 ka) is gray, clay-rich mud with angular pebbles, marked by oxidization near the top and is interpreted as glacial–lacustrine mud. Unit 2 (399–371 cm; 14.6–11.1 ka) is sandy mud, interpreted as lacustrine sediment with abundant hillslope-derived sediment. Unit 3 (371–0 cm; 11.1–0 ka), comprising 78% of the core, is dark-brown, silt- and organic-rich mud (gyttja) interpreted as lacustrine sediment of an increasingly productive lake. The pond is surrounded by dense *Alnus* thickets, and the sediment younger than 8 ka contains abundant leaf fossils, which were used for many of the ^{14}C analyses in Unit 3. With their short residence times on the landscape and their relatively large sample masses, these leaf fossils generated ^{14}C ages with a uniform downcore trend.

Three ^{14}C ages were analysed from Unit 1 (Table 2), but are not included in the age model for the core because they are from below a probable disconformity, and because no tephra beds were found in Unit 1. Two stratigraphically reversed ^{14}C ages of 12.6 and 12.2k cal a BP were obtained from Unit 2. The samples were separated by 4 cm and were prepared and analyzed on two occasions. A second pair of samples from the base of Unit 3, about 20 cm higher in the core, returned ^{14}C ages of 13.4 and 13.0k cal a BP (also stratigraphically reversed). Similarly, the samples were separated by 4 cm and were analyzed on two occasions. Rather than inferring that the younger material was somehow injected into older sediment, we prefer the more likely explanation that older material that overlies the younger ages was reworked. We therefore reject the older pair of ages. The age–depth model was extrapolated to the base of Unit 2, where it reaches 14.5 ± 0.6 ka. On this basis, the sedimentary sequence includes a period of non-deposition (with possible erosion) of about 6000 years, which is represented by an oxidized zone at the top of Unit 1.

Fifteen samples ranging from 10.0 to 0.2 ka (from 357 to 24 cm depth) were analyzed for ^{14}C from Unit 3. $^{239+240}$Pu, which was released into the atmosphere during nuclear weapons testing beginning in the early 1950 s, was not detected below 1 cm in the surface of Unit 3 (Fig. 3), suggesting the uppermost sediment in the surface core had been truncated, possibly during coring. Therefore, sediment ages for the top of LSP-3/4 are only poorly constrained, but the record probably begins in the 1950 s. We assigned an age of 1953 to the interval of 1.0–0.5 cm (Table 2). This age was combined with the 15 ^{14}C ages from Unit 3 and the two accepted ages from Unit 2 to derive an age–depth model (Fig. 2). The average uncertainty associated with this age model, as evaluated at 1-cm intervals between the surface and the lowest ^{14}C-dated level, is ± 109 a.

Sunday Pond

Sunday Pond (informal name) is located along the inflow to Sunday Lake in the north-central Ahklun Mountains. Core SP-1 comprises massive, organic-rich mud with six tephra beds (Feinberg, 2000; Levy, 2002). Five vegetation samples were analyzed from the lower half of the 4.8-m-long core for ^{14}C (Table 2). The ages range from 7.3 to 4.0k cal a BP and were taken from around the zone of multiple tephra beds. The age–depth model was extrapolated upward to the youngest tephra bed at 3.9 ka and downward to the oldest tephra bed at around 8.6 ka (Fig. 2). The average age uncertainty between the oldest and youngest ^{14}C-dated levels is ± 112 a, with larger uncertainties over the extrapolated intervals.

Little Swift Lake

Little Swift Lake is located in the north-central Ahklun Mountains. The sedimentary sequence, geochronology and fossil pollen assemblages from a 575-cm-long core (LS-A) were described by Axford and Kaufman (2004). The sediment includes three prominent tephra beds. We used the original eight ^{14}C ages (recalibrated here; Table 2) fitted to a smooth spline to derive an age–depth model, which is similar to the original regression-based model, while including an estimate of the age uncertainty (± 221 a average between the oldest and youngest ^{14}C-dated levels). As shown previously (Axford and Kaufman, 2004), the ^{14}C ages from Little Swift Lake are systematically and inexplicably too old, and we applied the prescribed 600 a offset to the tephra beds in this study.

Waskey Lake

Waskey Lake (informal name) is located in the north-eastern part of the Ahklun Mountains. Its headwaters encompass one of the highest and most extensively glaciated massifs in the range. The physical properties of the 6.6-m-long core WL-1 were studied previously to infer changes in glacier activity within the catchment (Levy *et al.*, 2004). The core contains three prominent tephra beds. The lower two were analyzed previously for their major-element geochemistry (Levy *et al.*, 2004). For consistency, we re-analyzed these tephra beds in this study, in addition to the upper tephra. Because core WL-1 is now largely consumed, however, we sampled the upper two tephra beds from core WL-2, which is described by Levy (2002). We used the original seven ^{14}C ages and the inferred offset with the lake floor based on correlation with the surface core (WL-1A; −50 cal a BP at 5 cm above the core top, Levy *et al.*, 2004) to construct a revised age model for the core (Fig. 3). The average age uncertainty over the modeled 11 100-year age range is ± 201 a.

Nimgun Lake

Nimgun Lake is located in the foothills of the south-western Ahklun Mountains. The segment from 3.4 to 5.0 m in core NL-2, which spans the last glacial–interglacial transition, was studied previously for its pollen assemblage and other paleoenvironmental indicators (Hu *et al.*, 2002). The lake was cored in 1996 and the cores have since been destroyed. The positions of five tephra beds across the 5.3-m-long core were determined from laboratory notes, and from MS and loss-on-ignition profiles. None of the tephra beds were available for this study. Instead, tephra correlations were based on similarity in age with other dated tephra beds. We used the six ^{14}C ages from the section that was previously analyzed (Hu *et al.*, 2002), and include an additional previously unpublished age from higher in the core (Table 2) to develop the age model (Fig. 3). The average age uncertainty for the interval between the oldest and youngest ^{14}C-dated levels is ± 133 a.

Arolik Lake

Arolik Lake is located beyond the late Wisconsinan ice limit, 24 km south-west of Nimgun Lake. The lake yielded the longest cores yet recovered from the Ahklun Mountains, up to 8.6 m long and extending to 35.8 ka, based on revised calibrations using IntCal09 (Reimer *et al.*, 2009). Visually apparent tephra layers, all associated with peaks in MS, were correlated among four cores taken from across the lake, and were assigned letter designations, 'Tephra A' through 'Tephra F' from youngest to oldest (Kaufman *et al.*, 2003). Of the cores, AL-4 contained the most macrofossils for ^{14}C analysis and the longest sedimentary sequence. The original 17 ^{14}C ages (Table 2) were recalibrated and fitted to a smooth spline to develop the age model (Fig. 3). The average age uncertainty for the interval between the oldest and youngest ^{14}C-dated levels is ± 316 a.

Tephra descriptions, geochemistry and geochronology

Twenty-four tephra beds were analyzed from the six lakes (Fig. 4). In addition, three beds were analyzed from each of two lakes in the region (Sunday and Cascade lakes) that lack ^{14}C age control, and two from a soil pit near Cascade Lake. The stratigraphic level, thickness, age and general physical properties of each tephra sample are detailed in Table 3. Typical glass shard morphologies are shown in Fig. 5.

Of the 26 radiocarbon-dated tephra beds at the six lakes and from the soil pit, seven can be correlated between two or more

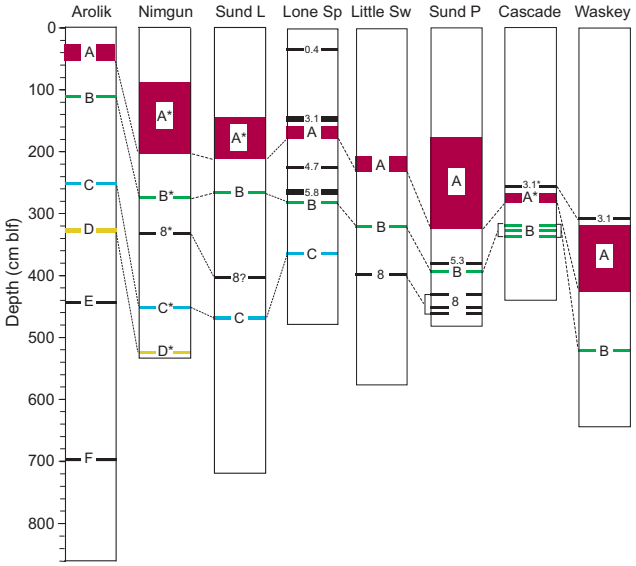

Figure 4. Simplified stratigraphic sequences showing depths, thicknesses and correlations among visually prominent tephra beds in sediment cores from eight study lakes. Asterisks indicate beds that were not analyzed for geochemistry. Arolik, Arolik Lake core AL-4; Nimgun, Nimgun Lake core NL-2; Sund L, Sunday Lake core SL-1; Lone Sp, Lone Spruce Pond core 07-LSP-3; Little Sw, Little Swift Lake core LS-A; Sun P, Sunday Pond core SP-1; Cascade, Cascade Lake core CA -2; Waskey, Waskey Lake cores WL-1 and WL-2. This figure is available in colour online at wileyonlinelibrary.com.

sites on the basis of their ^{14}C ages (Table 4). At least five of the other beds appear to be present at only one site based on their unique age. Some cores have been destroyed and the tephras are no longer available, in which case we present likely correlations based only on their modeled ages.

The major-element geochemistry of glass shards from most of the tephra beds supports the tentative ^{14}C-based correlations and the interpretation that they are from different eruptions (Table 5), with the possible exception of the 3.1- and 0.4-ka tephra beds discussed below. In general, the normalized major-element geochemistry of glass from the tephra beds ranges from basaltic andesite to rhyolite, with some grains transitioning to trachyandesite and trachydacite. The major-element compositions of each of the tephra beds is summarized in Table 6 and the composition of individual grains is listed in Supporting information (Table S1). Most of the tephra beds have unimodal geochemical populations, although some have 'tails' trending towards higher SiO_2 weight percent (wt%) values. Tephra A and three other beds exhibit distinctly bimodal populations: a rhyolitic mode and an andesitic to basaltic–andesitic mode (Fig. 6). The thickest tephra deposits provided high-quality and plentiful analyses. Many thinner beds (UA 1787, 2001, 2003, 2004, 2005, 2006) contain substantial amounts of detrital glass, making it more difficult to discern a distinct geochemical population(s). This suggests the lake sediment with relatively high MS values can contain abundant detrital glass.

From oldest to youngest, the tephra beds include the following.

Tephra F

This tephra is no longer available for analysis. Its age in Arolik Lake is 25.4 ± 0.4 ka.

Tephra E

This bed (UA 1795) was originally named as part of the sequence from Arolik Lake (Kaufman *et al.*, 2003). Its revised

Table 3. Tephra bed ages and physical characteristics.

Core ID	Lab ID (UA)	Bottom depth (cm)		Thickness (cm)	Age (cal a BP)	Description
		Tube	Tephra-free			
Lone Spruce Pond						
09-LSP-4A	1966	34.2	34.0	0.2	377 ± 62	Bubble-walled and tricuspate shards, some blocky glass
07-LSP-3	1964	149.5	165.2	7.1	3113 ± 72	Bubble-walled and tricuspate shards, some blocky glass
07-LSP-3	1963	175.0	172.7	18.0	3414 ± 72	Bubble-walled and tricuspate shards, some blocky glass
07-LSP-3	1965	223.2	220.7	0.2	4745 ± 133	Bubble-walled and tricuspate shards, some blocky glass
07-LSP-3	1783	271.0	254.2	14.5	5788 ± 89	Bubble-walled and tricuspate shards, some blocky glass
07-LSP-3	1786	281.0	261.5	2.5	6021 ± 74	Blocky pumice, generally crystal-rich, some bubble-walled and tricuspate shards
07-LSP-3	1785	363.0	342.7	1.0	13002 ± 410	Blocky pumice, crystal-rich
Sunday Pond						
SP-1	1780	327.0	180.0	147.0	3874 ± 192	Bubble-walled and tricuspate shards, some blocky glass
SP-1	2002	381.0	233.0	1.0	5349 ± 127	Mixed morphology, predominantly crystal-rich blocky glass
SP-1	1796, 2003	392.5	244.0	0.5	5897 ± 125	Blocky pumice, generally crystal-rich, some bubble-walled and tricuspate shards
SP-1	2004	432.0	282.5	1.0	7548 ± 113	Mixed morphology
SP-1	2005	451.0	301.0	0.5	8230 ± 278	Mixed morphology
SP-1	1787, 2006	461.0	310.5	0.5	8580 ± 637	Mixed morphology
Little Swift Lake*						
LS-A	1967	232.0	208.0	24.0	3799 ± 112	Bubble-walled and tricuspate shards, some blocky glass
LS-A	1794	318.5	294.0	0.5	5835 ± 155	Blocky pumice, generally crystal-rich, some bubble-walled and tricuspate shards
LS-A	1784	398.5	373.5	0.5	7995 ± 316	Mixed morphology
Waskey Lake†						
WL-2	1793	310	310	1	3097 ± 271	Bubble-walled and tricuspate shards, some blocky glass
WL-1	1968	425	320	105	3573 ± 233	Bubble-walled and tricuspate shards, some blocky glass
WL-1	1788	524.0	377.0	2.0	6467 ± 235	Blocky pumice, generally crystal-rich, some bubble-walled and tricuspate shards
Arolik Lake‡						
AL-6	1970	185	185	16	3434 ± 142	Bubble-walled and tricuspate shards, some blocky glass
AL-6	1969	241	224	1	5988 ± 169	Blocky pumice, generally crystal-rich, some bubble-walled and tricuspate shards
AL-4	1791	255	226	1	12231 ± 276	Blocky pumice, crystal-rich
AL-4	1781	332	295	8	15817 ± 182	Mix of blocky and frothier pumice, some crystal-rich
AL-4	1795	445	407	1	18665 ± 223	Blocky pumice, glass shards
AL-4	—	700.5	662	0.5	25371 ± 409	Not available
Nimgun Lake						
NL-2	—	206	91	115	4013 ± 101	Not available
NL-2	—	278	161	2	6408 ± 191	Not available
NL-2	—	335	217	1	8142 ± 133	Not available
NL-2	—	455	336	1	12501 ± 159	Not available
NL-2	—	528	408	1	15193 ± 356	Not available
Sunday Lake						
SL-1	—	215.0	148.0	67.0	—	Not available
SL-1	1792	269.5	194.0	0.5	—	Blocky pumice, generally crystal-rich, some bubble-walled and tricuspate shards
SL-1	1790	408.0	331.5	1.0	—	Mixed morphology
SL-1	1789	473.0	394.5	2.0	—	Blocky pumice, crystal-rich
Cascade Lake						
CA-2	—	259.0	257.9	1.0	—	Not available
CA-2	—	285.0	268.9	15.0	—	Not available
CA-2	1971	324.0	304.9	3.0	—	Mixed morphology
CA-2	1972	333.0	314.4	2.5	—	Blocky pumice, generally crystal-rich, some bubble-walled and tricuspate shards
CA-2	1973	341.0	320.4	1.0	—	Mixed morphology
Cascade soil pit lenses						
—	1779, 1974	4.3	—	2.0	—	Bubble-walled and tricuspate shards, some blocky glass
—	1975	15	—	Top	—	Bubble-walled and tricuspate shards, some blocky glass
—	1976	18	—	Middle	—	Bubble-walled and tricuspate shards, some blocky glass
—	1977	22	—	Bottom	—	Bubble-walled and tricuspate shards, some blocky glass

Note: Ages are cal a BP (BP); age uncertainties (±) are one half of the 95% confidence intervals determined by *clam* (see text). * Ages of tephra from Little Swift lake include a 600-year adjustment as described by Axford and Kaufman (2004). † Ages of tephra from WL-2 are projected from WL-1 (see Levy *et al.*, 2004). ‡ Ages of tephra from AL-6 are projected from AL-4 (see Kaufman *et al.*, 2003).

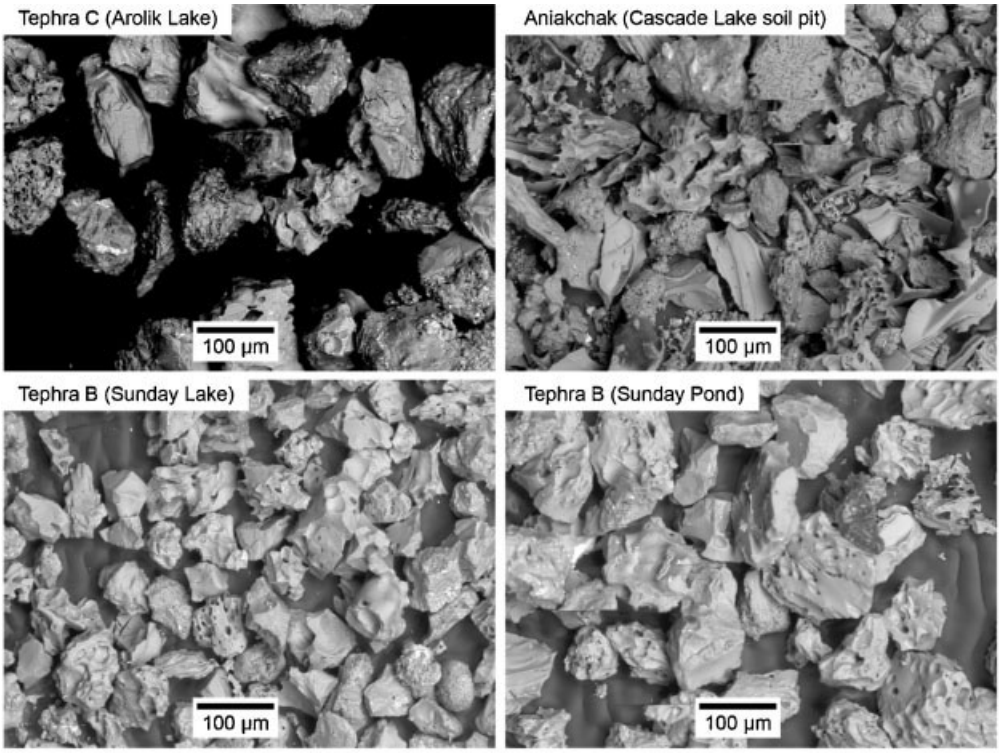

Figure 5. Scanning electron micrographs of tephra grains. Tephra A (Aniakchak tephra) is predominantly bubble-wall and tri-cuspate shards, with some thick-walled pumice marked by large vesicles. Tephra B and Tephra C are both predominantly chunky pumice with abundant phenocrysts and microcyrsts, which complicate analysis of their geochemistry. Tephra B includes some microcryst-free bubble-wall shards and thick-walled pumice.

age is 18.7 ± 0.2 ka. No other sediment core from the region extends back this far and the tephra has not been found elsewhere. This tephra bed can be distinguished by its K_2O content, which is distinctly lower than any other tephra in this study (Fig. 6).

Tephra D

This bed (UA 1781) was originally named as part of the sequence from Arolik Lake (Kaufman *et al.*, 2003). Its age overlaps with that of a prominent tephra in nearby Nimgun Lake (not analyzed). The mean of the two ages is 15.5 ± 0.3 ka. Tephra D contains highly vesicular pumice and lacks tri-cuspate and bubble-wall shards. The geochemistry of Tephra D is very similar to that of Tephra B, but with less scatter, and can be clearly distinguished by its Al_2O_3, FeO_t and K_2O contents (Fig. 6).

Tephra C

This bed (UA 1791) was originally named as part of the sequence from Arolik Lake (Kaufman *et al.*, 2003). Its age overlaps with that of a prominent tephra in Nimgun Lake (not analyzed), and with the lowest tephra in Lone Spruce Pond (UA 1785). The mean of the three ages is 12.6 ± 0.4 ka. Tephra C is composed entirely of crystal-rich blocky glass and pumice (Fig. 5). It contains both brown and clear glass. Other than the low SiO_2 mode of Tephra A, Tephra C has the lowest SiO_2 of any of the Ahklun Mountain tephra beds. It has distinct TiO_2, FeO_t and Al_2O_3 contents.

8-ka tephra

This bed is best expressed in Little Swift Lake (UA 1784), where it is dated to about 8 ka. Its age overlaps with that of a prominent tephra in Nimgun Lake (not analyzed), and with all three of the

Table 4. Tephra beds and their ages (cal a BP) based on ^{14}C-constrained sedimentation rate models.

Tephra	Lone Spruce Pond	Sunday Pond	Nimgun Lake	Waskey Lake	Little Swift Lake	Arolik Lake	Cascade test pit*	Mean age
0.4 ka	377 ± 62	—	—	—	—	—	505 ± 20	441 ± 64
3.1 ka	3113 ± 72	—	—	3097 ± 271	—	—	—	3105 ± 8
Aniakchak	3414 ± 72	3874 ± 192	4013 ± 101	3573 ± 233	3799 ± 112	3434 ± 142	—	3685 ± 101
LSP 4.7 ka	4745 ± 133	—	—	—	—	—	—	—
SP 5.3 ka	—	5349 ± 127	—	—	—	—	—	—
LSP 5.8 ka	5788 ± 89	—	—	—	—	—	—	—
Tephra B	6021 ± 74	5897 ± 125	6408 ± 191	6467 ± 235	5835 ± 155	5988 ± 169	—	6103 ± 110
8 ka	—	—	8142 ± 133	—	7995 ± 316	—	—	8069 ± 74
Tephra C	13002 ± 410	—	12501 ± 159	—	—	12231 ± 276	—	12366 ± 135
Tephra D	—	—	15193 ± 356	—	—	15817 ± 182	—	15505 ± 312
Tephra E	—	—	—	—	—	18665 ± 223	—	—
Tephra F	—	—	—	—	—	25371 ± 409	—	—

LSP, Lone Spruce Pond; SP, Sunday Pond. Note: Ages are cal a BP (BP); age uncertainties (±) are one half of the 95% confidence intervals determined by *clam* (see text). *^{14}C age from below tephra bed.

Table 5. Tephra beds with provisional correlations listed by University Alberta (UA) laboratory numbers.

Tephra	Lone Spruce Pond	Sunday Pond	Waskey Lake	Little Swift Lake	Arolik Lake	Cascade Lake	Sunday Lake
0.4 ka	1966	—	—	—	—	1779 = 1974*	—
3.1 ka	1964	—	1793	—	—	—	—
Aniakchak	1963	1780	1968	1967	1970	1975, 1976, 1977*	—
LSP 4.7 ka	1965	—	—	—	—	—	—
SP 5.3 ka	—	2002	—	—	—	—	—
LSP 5.8 ka	1783	—	—	—	—	1971?	—
Tephra B	1786	1796 = 2003	1788	1794	1969	1972 or 1973?	1792
8 ka	—	2004, 2005 or 2006	—	1784	—	—	1790?
Tephra C	1785	—	—	—	1791	—	1789
Tephra D	—	—	—	—	1781	—	—
Tephra E	—	—	—	—	1795	—	—

LSP, Lone Spruce Pond; SP, Sunday Pond. *Sampled from a soil pit near Cascade Lake.

lowest tephra in Sunday Pond (UA 2004, 2005 and 2006 = 1787). The geochemical data from the Sunday Pond tephra are sparse and heterogeneous, and we are uncertain which of the three beds correlates with the 8-ka tephra from the other two sites, although UA 2004 contains several shards with compositions similar to UA 1784 (Table S1). The mean age of the tephra, based on Little Swift and Nimgun lakes, is 8.1 ± 0.1 (1σ) ka. Its geochemical composition plots between Tephra B and Tephra A, and is similar to the higher SiO_2 'tail' of Tephra B (pop. 2, Table 6), and the few shards from Tephra A that fall between its modal populations. UA 1790, from Sunday Lake, is geochemically similar to UA 1784, but the two appear to differ in MnO (Fig. 7). With such few analyses, this difference is not sufficient to distinguish the two tephra conclusively, but the difference is likely real. The core from Sunday Lake lacks age control to determine the age of this possibly unique tephra bed.

Tephra B

This bed (UA 1969) was originally named as part of the sequence from Arolik Lake (Kaufman *et al.*, 2003). Along with Tephra A, it is the most widespread of all of the regional tephra beds. Its age overlaps with those of a prominent tephra in all five other lakes, including Nimgun Lake (not analyzed), Lone Spruce Pond (UA 1786), Sunday Pond (UA 1796 = 2003), Waskey Lake (UA 1788) and Little Swift Lake (UA 1794). The mean of the six ages is 6.1 ± 0.3 (1σ) ka. Levy *et al.* (2004) also analyzed the major-element geochemistry of Tephra B from Waskey Lake, and their results are similar. Tephra B is predominantly blocky glass and pumice, with rare bubble-walled shards and large vesicular pumice. Many of the glass shards are crystal-rich, containing microcrysts of plagioclase and pyroxene. The glass tends to be various shades of brown, with rare clear glass. Tephra B glass geochemistry is largely andesitic, and overlaps with Tephra D, although the two are distinguishable by their Al_2O_3, FeO_t and K_2O (Fig. 6). Tephras with similar geochemistry and corresponding stratigraphic position were analyzed from Sunday Lake (UA 1792) and from Cascade Lake (UA 1972), but neither of the cores was dated. UA 1971 and UA 1973, which bracket UA 1972, also contain a geochemical population that correlates with Tephra B, but include other geochemical populations (including Aniakchak-like material) and are glass-poor. These results suggest that Tephra B in these samples may have been reworked from UA 1972, which is separated from UA 1971 and 1973 by less than 10 cm.

Lone Spruce Pond 5.8-ka tephra

This bed (UA 1783) is known only from Lone Spruce Pond where it forms the thickest tephra layer (14.5 cm) other than Tephra A (18.0 cm). Its age (5.8 ± 0.1 ka) is consistent with a correlation with Tephra B, but its major-element geochemistry is bimodal and indistinguishable from Tephra A (Fig. 8). However, its trace-element geochemistry is distinct from Tephra A, particularly with high-field-strength elements such as Zr, Nb, Y and rare earth elements (REE) in the rhyolitic fraction (see supporting Table S2). These differences are apparent in the chondrite-normalized REE profiles (Fig. 9).

Sunday Pond 5.3-ka tephra

This bed (UA 2002) is known only from Sunday Pond, where it is dated at 5.3 ± 0.1 ka. Like other relatively thin and diffuse tephra beds, the geochemical composition has several populations, including one that overlaps with Tephra B. The predominant population is distinct from Tephra B, however, with lower Al_2O_3 and higher FeO_t (Fig. 7).

Lone Spruce Pond 4.7-ka tephra

This thin bed (UA 1965; 0.2 cm thick) is known only from Lone Spruce Pond, where it is dated at 4.7 ± 0.1 ka. The tephra bed is composed predominantly of pumice with large vesicles, and some blocky pumice; tricuspate and bubble-wall shards are present, but in lower abundance than in Tephra A. Its geochemistry is similar to the high SiO_2 population of Tephra A, but can be differentiated by its K_2O, Al_2O_3 and Cl (Fig. 6).

Tephra A (Aniakchak tephra)

This bed (UA 1970) was originally named as the uppermost in the sequence from Arolik Lake where it was correlated with the caldera-forming eruption of Aniakchak volcano of the same age (Kaufman *et al.*, 2003). The tephra comprises the thickest bed in all lakes from the region, and is essentially ubiquitous in outcrops and soil pits across the landscape. Levy *et al.* (2004) presented geochemical evidence from Waskey Lake sediments for its correlation with Aniakchak volcano. The widespread distribution of the Aniakchak tephra across western Alaska has been described previously (Reihle *et al.*, 1987; Begét *et al.*, 1992). The tephra has also been identified in ice cores from Greenland, where it was recovered from the 3595 ± 4 cal a BP layer (1642 BC; Pearce *et al.*, 2004; Denton and Pearce, 2008). The thickest tephra beds are of similar ages in all other lakes including Nimgun Lake (not analyzed and somewhat older than expected), Lone Spruce Pond (UA 1963), Sunday Pond (UA

Table 6. Summary of major-element geochemistry of tephra beds.

	Geochemistry of tephra beds (wt%, Mean ± SD)*											
Sample	SiO_2	TiO_2	Al_2O_3	FeO_t	MnO	MgO	CaO	Na_2O	K_2O	Cl	H_2O_{diff}	*n*
Aniakchak (Reference data)												
Pop. 1	59.21 ± 1.77	1.35 ± 0.09	16.63 ± 0.23	7.51 ± 0.97	0.22 ± 0.03	2.76 ± 0.39	6.20 ± 0.81	4.42 ± 0.39	1.59 ± 0.21	0.12 ± 0.04	2.60 ± 1.40	16
Pop. 2	71.15 ± 0.27	0.49 ± 0.04	15.24 ± 0.14	2.48 ± 0.10	0.14 ± 0.03	0.51 ± 0.03	1.75 ± 0.09	5.13 ± 0.28	2.95 ± 0.10	0.19 ± 0.03	2.32 ± 1.92	43
Tephra A (Aniakchak)												
Pop. 1	59.02 ± 1.45	1.37 ± 0.09	16.50 ± 0.26	7.59 ± 0.76	0.21 ± 0.04	2.81 ± 0.33	6.41 ± 0.60	4.42 ± 0.38	1.55 ± 0.18	0.12 ± 0.03	2.51 ± 1.25	183
Pop. 2	71.09 ± 0.60	0.49 ± 0.06	15.17 ± 0.18	2.53 ± 0.26	0.14 ± 0.04	0.51 ± 0.08	1.81 ± 0.20	5.12 ± 0.33	2.95 ± 0.11	0.20 ± 0.03	2.51 ± 1.61	301
5.8-ka tephra												
Pop. 1	59.61 ± 1.25	1.36 ± 0.07	16.49 ± 0.24	7.43 ± 0.70	0.20 ± 0.04	2.72 ± 0.29	6.31 ± 0.56	4.21 ± 0.43	1.55 ± 0.14	0.12 ± 0.03	2.00 ± 0.76	42
Pop. 2	71.23 ± 0.32	0.50 ± 0.04	15.09 ± 0.22	2.51 ± 0.10	0.15 ± 0.03	0.50 ± 0.04	1.75 ± 0.09	5.03 ± 0.20	3.08 ± 0.12	0.19 ± 0.03	1.74 ± 1.45	33
3.1-ka tephra												
Pop. 1	58.99 ± 1.26	1.37 ± 0.09	16.40 ± 0.24	7.61 ± 0.60	0.21 ± 0.04	2.79 ± 0.34	6.47 ± 0.55	4.46 ± 0.37	1.56 ± 0.23	0.13 ± 0.03	2.65 ± 0.92	50
Pop. 2	71.17 ± 0.38	0.48 ± 0.05	15.11 ± 0.20	2.52 ± 0.08	0.14 ± 0.03	0.49 ± 0.04	1.81 ± 0.09	5.12 ± 0.33	2.97 ± 0.11	0.20 ± 0.03	2.74 ± 1.71	69
0.4-ka tephra												
Pop. 1	59.76 ± 1.77	1.28 ± 0.14	16.32 ± 0.37	7.45 ± 1.00	0.21 ± 0.04	2.62 ± 0.40	6.17 ± 0.82	4.42 ± 0.46	1.66 ± 0.26	0.12 ± 0.03	2.21 ± 0.88	27
Pop. 2	71.08 ± 0.65	0.50 ± 0.07	15.14 ± 0.16	2.53 ± 0.27	0.14 ± 0.04	0.52 ± 0.09	1.85 ± 0.25	5.08 ± 0.35	2.96 ± 0.11	0.20 ± 0.03	2.64 ± 1.45	96
Tephra B												
Pop. 1	61.99 ± 0.48	1.17 ± 0.07	15.77 ± 0.18	7.46 ± 0.27	0.21 ± 0.04	1.93 ± 0.10	4.92 ± 0.20	4.73 ± 0.24	1.68 ± 0.08	0.13 ± 0.03	2.15 ± 1.33	384
Pop. 2	66.97 ± 0.54	0.71 ± 0.05	15.44 ± 0.19	5.40 ± 0.23	0.20 ± 0.04	0.84 ± 0.07	2.88 ± 0.18	5.17 ± 0.26	2.25 ± 0.07	0.16 ± 0.03	1.59 ± 0.85	12
Tephra C	59.02 ± 1.12	1.75 ± 0.15	15.40 ± 0.46	9.25 ± 0.50	0.25 ± 0.03	2.44 ± 0.33	5.70 ± 0.47	4.30 ± 0.34	1.77 ± 0.27	0.15 ± 0.03	2.12 ± 1.13	74
Tephra D	61.34 ± 0.56	1.24 ± 0.06	16.38 ± 0.25	7.10 ± 0.26	0.18 ± 0.04	2.28 ± 0.14	5.18 ± 0.27	4.47 ± 0.45	1.75 ± 0.09	0.12 ± 0.03	1.86 ± 0.86	16
Tephra E	62.94 ± 2.17	1.16 ± 0.15	15.45 ± 0.37	7.28 ± 0.85	0.16 ± 0.02	1.99 ± 0.46	4.93 ± 0.72	4.69 ± 0.25	1.30 ± 0.17	0.12 ± 0.03	0.58 ± 1.16	8
Lone Spruce												
4.7 ka	71.54 ± 0.76	0.44 ± 0.08	14.85 ± 0.24	2.62 ± 0.30	0.13 ± 0.04	0.42 ± 0.11	1.64 ± 0.26	4.95 ± 0.33	3.23 ± 0.18	0.18 ± 0.02	3.41 ± 2.02	47
Little Swift												
8 ka	67.05 ± 0.97	0.83 ± 0.16	15.10 ± 0.12	5.25 ± 0.33	0.17 ± 0.05	0.91 ± 0.19	2.97 ± 0.37	5.00 ± 0.16	2.56 ± 0.14	0.16 ± 0.02	3.95 ± 2.54	8
Sunday Lake												
8 ka?	66.55 ± 1.15	0.86 ± 0.11	15.14 ± 0.31	5.42 ± 0.41	0.29 ± 0.06	0.98 ± 0.19	3.19 ± 0.41	4.95 ± 0.35	2.47 ± 0.16	0.14 ± 0.03	2.02 ± 0.67	10
Sunday Pond												
5.3 ka	61.49 ± 0.46	1.22 ± 0.06	15.37 ± 0.10	8.08 ± 0.22	0.20 ± 0.03	1.89 ± 0.10	5.06 ± 0.27	4.83 ± 0.28	1.73 ± 0.12	0.13 ± 0.02	2.49 ± 1.85	10

* Data are normalized to 100 wt% on a water-free basis; SD, standard deviation; averages include zero values; *n*, umber of analyses; FeO_t, total Fe as FeO; H_2Odiff, water by difference. Standardization by mineral and glass standards.

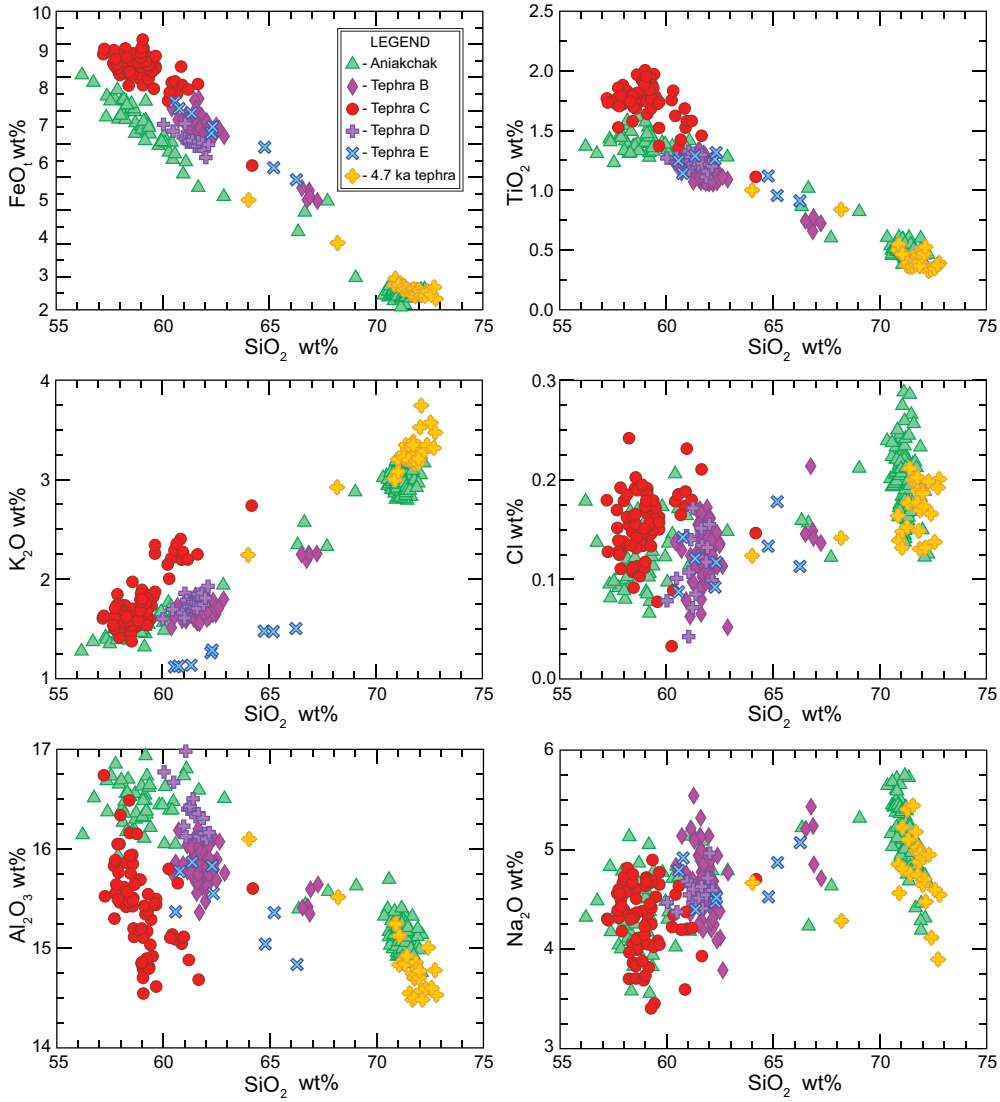

Figure 6. Bivariate plots of glass major-element geochemistry of the most widespread and geochemically distinct tephra beds analyzed in this study. The oxides presented are those that most clearly distinguish the tephra beds. Five of these tephra beds, Tephras B, C, D and E and Lone Spruce Pond 4.7-ka tephra, have not been described elsewhere. Data are given in Table S1 and summarized in Table 6. This figure is available in colour online at wileyonlinelibrary.com.

1780), Waskey Lake (UA 1968) and Little Swift Lake (UA 1967). The mean of the six ages is 3.7 ± 0.2 (1σ) ka. The bed was also subsampled and analyzed for this study from three levels in a soil pit near Cascade Lake (UA 1975, 1976, 1977).

Tephra A contains a high percentage of bubble-wall and tricuspate shards, platy glass, elongate pumice, and pumice with large vesicles. Less common are blocky glass and pumice, which are occasionally crystal-rich. Brown and clear glass shards are present in roughly the same proportion. Geochemically, the tephra is distinct in its bimodal population, with differences in SiO_2 content of more than 10 wt%. Of hundreds of distal tephra analyzed in the Yukon and Alaska, only several have such a widely separated bimodal population (B. J. L. Jensen, unpublished data).

3.1-ka tephra

This tephra was sampled from Lone Spruce Pond (UA 1964) and from Waskey Lake (UA 1793), where the beds overlap in age and are stratigraphically above the Aniakchak tephra. The age of this bed in both cores is ~3.1 ka. The major-element geochemistry of this tephra is indistinguishable from the Aniakchak tephra. Because of the similarity, we also analyzed the trace-element geochemistry of this bed to determine if it was distinct from the Aniakchak tephra (Table S2, Fig. 9). The bed comprises pure glass shards in both lakes, and an undated but possibly correlative bed is also found in Cascade Lake (neither analyzed nor dated).

0.4-ka tephra

This tephra was sampled from Lone Spruce Pond (UA 1966) and from the soil pit near Cascade Lake (UA 1779 = 1974). The mean of the two ages is 0.4 ± 0.1 (1σ) ka. Similar to the 3.1-ka tephra, the major- and trace-element geochemistry of this tephra is indistinguishable from Aniakchak tephra. The tephra layer appears to be widespread across the landscape, directly below the surface organic mat and capping a buried A/B soil horizon. It is typically separated from the underlying Aniakchak tephra by centimeters to decimeters of loess or other non-volcanic sediment. The sample from Lone Spruce Pond (UA 1966) also contains abundant detrital glass (Table S1).

Discussion

Age uncertainties

The tephra beds can be used as chronostratigraphic markers to evaluate the reliability of the age–depth models of lake cores, and the extent to which their confidence intervals are reliable indicators of the uncertainty of a given event. For this assessment, we assume that the true age of a tephra bed that

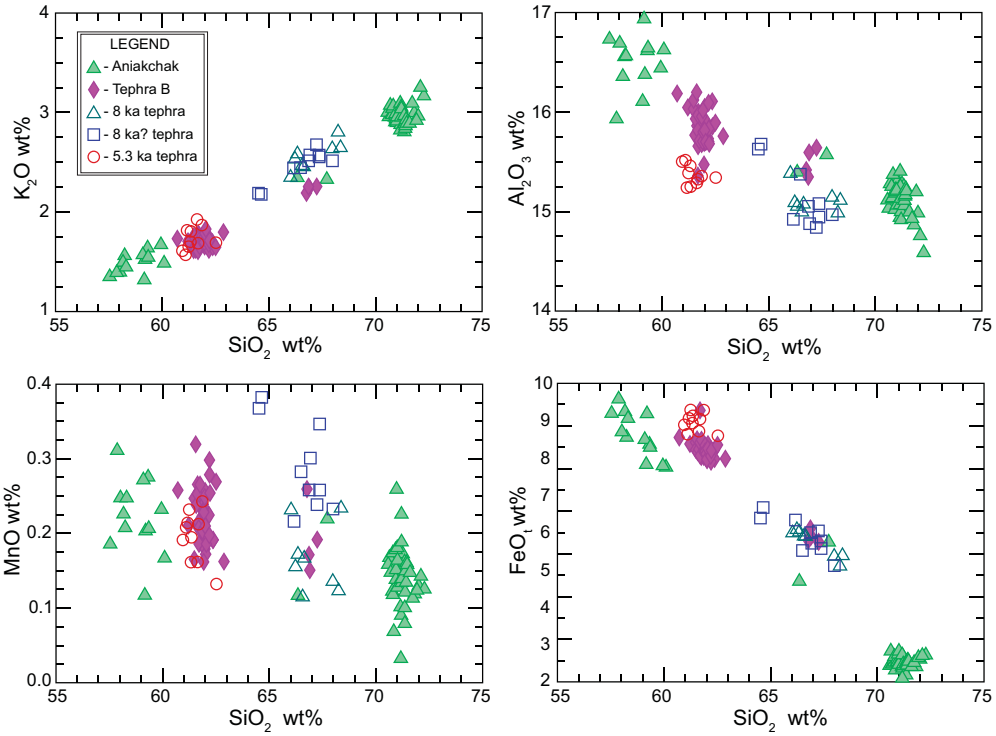

Figure 7. Bivariate plots of glass major-element geochemistry of the remaining three unique tephra beds presented in this study. Tephra A (Aniakchak tephra) and Tephra B are included for comparison. UA 1790, 1784 and 2002 contain other geochemical populations, mostly scattered and interpreted as detrital glass; the data in the diagrams are of the dominant mode. Data are listed in Table S1 and summarized in Table 6. This figure is available in colour online at wileyonlinelibrary.com.

was dated in different lakes falls within the $\pm 1\sigma_x$ of their mean age, and we compare this age with the confidence intervals of the age–depth models. The confidence intervals generated by the *clam* code are commensurate with the uniformity of the down-core trends and with the uncertainty in calendar-year calibrations of the ^{14}C ages. The average 2σ confidence interval for the age models from the six lakes in this study was 182 ± 81 a, as evaluated at 1-cm intervals over the dated ranges of the cores (Table 1). Age uncertainties increased where age models are extrapolated beyond the ^{14}C age control, and where ^{14}C ages are stratigraphically reversed. Age errors also increased with increasing age and for cores with fewer dated levels. Age uncertainties for individual tephra beds dated in this study ranged broadly (from ± 62 to ± 637 a), and averaged ± 199 a (Table 3), similar to the overall uncertainty of the age–depth models. The age errors for the tephra would be reduced if multiple ^{14}C ages were analyzed from directly above and below each bed, which can be difficult.

Because some tephra beds were dated in more than one lake, their ages can be determined as the average of the multiple

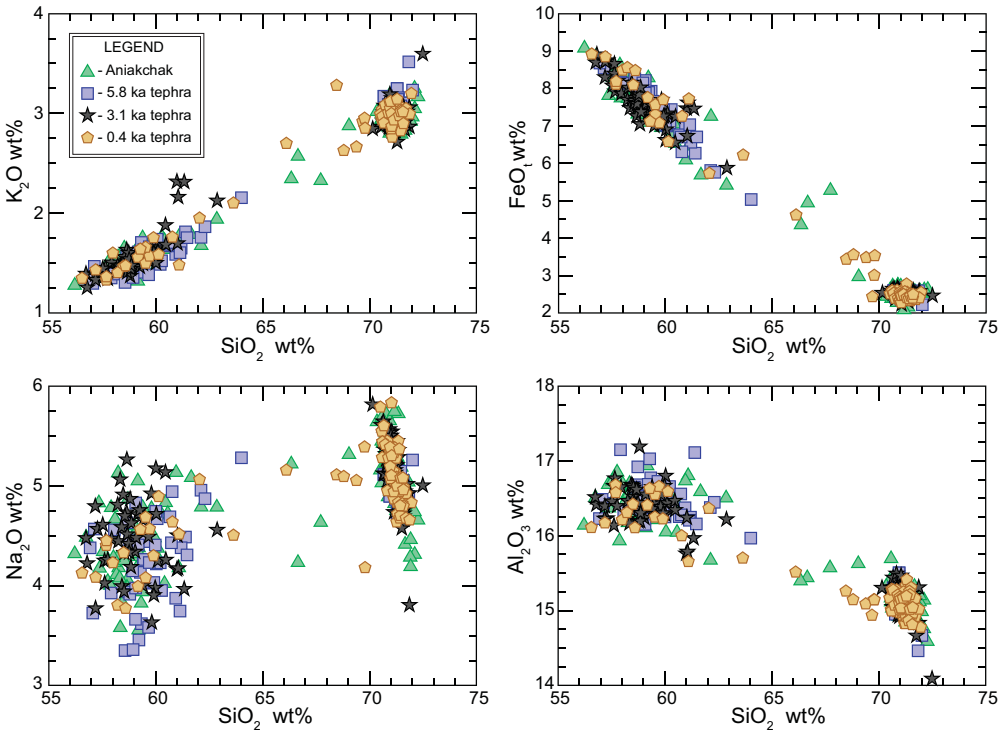

Figure 8. Bivariate plots of glass major-element geochemistry of tephra beds with distinct bimodal composition, similar to Tephra A (Aniakchak tephra) analyzed in this study. Oxides of Al, Na and Fe are displayed because during fractional crystallization they are depleted by different sets of minerals, and thus most likely indicate any differences in the geochemistry of each tephra bed. K_2O is included because this oxide has proven to be a useful discriminator in previous analyses of Alaskan tephra beds (Jensen *et al.*, 2008). These plots indicate that the major-element geochemistry cannot clearly distinguish among these tephra beds. There appears to be a slight variation between the 5.8-ka tephra bed (particularly with Na_2O) and the other beds. This could be an artifact of too few analyses, but trace-element geochemistry shows this is a unique bed. Data are listed in Table S1 and summarized in Table 6. This figure is available in colour online at wileyonlinelibrary.com.

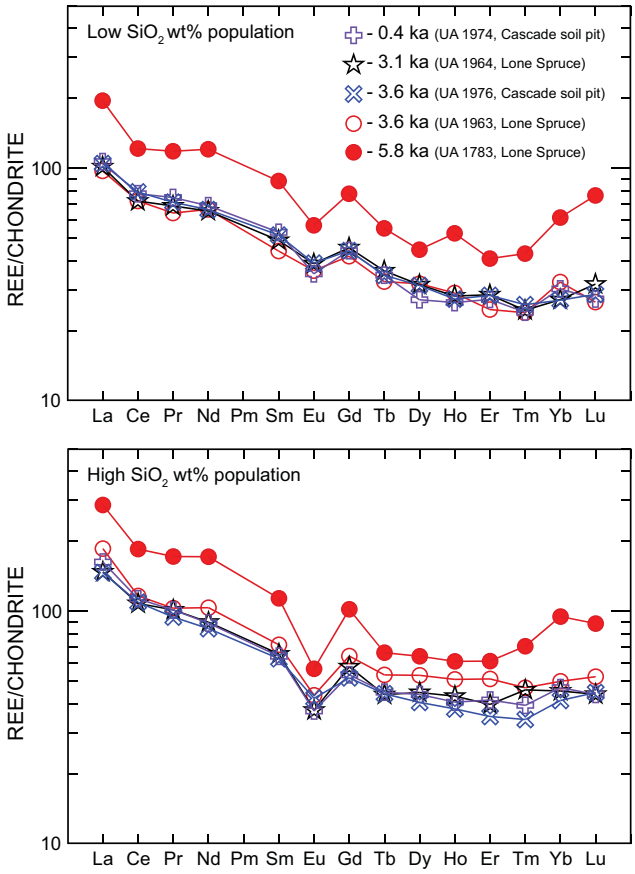

Figure 9. Trace element geochemistry of Aniakchak tephra and samples with major-element geochemistry that is indistinguishable from Aniakchak tephra. Rare earth element (REE) abundance plots are normalize to chondrite following Sun and McDonough (1989). This figure is available in colour online at wileyonlinelibrary.com.

occurrences, and their age uncertainties can be estimated by the standard errors of their means (Table 4). The $1\sigma_x$ for the seven tephra beds that were dated at more than one site averages ± 115 a. In nearly all cases, the confidence intervals derived from the age–depth model overlap in the mean age of the tephra within $1\sigma_x$ (Fig. 10). This indicates that the confidence intervals associated with the age–depth models are reliable indicators of the actual reproducibility of the specific event ages as dated at different sites.

Complexities of the tephrostratigraphy

Lakes are useful repositories for tephra because their sediment accumulates nearly continuously and organic material for radiocarbon dating is typically present. Lakes are not perfect recorders of tephra-fall history, however. The results of this study are consistent with others in showing that the sediment of different lakes within the same region can contain different tephrostratigraphies (e.g. Lowe, 2011). A variety of geomorphological processes and physiographic features within the catchment, as well as a range of limnologic and sedimentologic factors within the lake, can result in differential preservation and quality of the tephra record (e.g. de Fontaine *et al.*, 2007; Pyne-O'Donnell, 2011). In this study, 26 visible tephra beds were radiocarbon dated at six lakes, which are separated by 125 km. Of these, only two tephra beds were found in all lakes, while seven could be correlated between two or more sites based on their ages.

The major- and trace-element geochemistries of the 3.1- and 0.4-ka tephra beds are indistinguishable from the thickest and most widespread tephra in the region, the Aniakchak tephra (Fig. 8). These beds overlie the Aniakchak tephra, and they may comprise shards reworked from it. On the other hand, the beds comprise relatively pure tephra, appear to be conformable in the sedimentary sequence and are of indistinguishable age in different lakes. If they are reworked, then we speculate that they date to an interval of landscape destabilization during which the down-cutting of rivers and denudation of hillslopes exposed fresh outcrops of the thick tephra. Alternatively, the 3.1- and 0.4-ka tephra beds could be primary deposits erupted from Aniakchak volcano subsequent to the 3.7 ± 0.2 ka eruption of Tephra A, even though their major and trace-element geochemistry is indistinguishable. Neal *et al.* (2001) recognized at least six widespread tephra deposits from explosive eruptions of Aniakchak volcano that occurred following the caldera-forming eruption, including two events that occurred around 0.4 ka. The SiO_2 data presented by Browne *et al.* (2004) indicate that the geochemistry of the 0.4-ka tephra from Half Cone is similar, but not identical, to the Aniakchak tephra.

The 5.8-ka tephra from Lone Spruce Pond also has a bimodal geochemistry that is largely indistinguishable from Tephra A (Fig. 8), but underlies Tephra A. Despite the similarity in the major-element composition, the trace-element geochemistry clearly distinguishes this bed from Tephra A (Fig. 9). Neal *et al.* (2001) recognized evidence for at least 12 explosive eruptions at Aniakchak volcano between about 10 and 5 ka, including Miller and Smith's (1987) possible early caldera-forming event. Dreher *et al.* (2005) showed that the pre-caldera events have similar geochemistry to the caldera-forming event, but can be distinguished, particularly by the trace-element composition. A full comparison with their results is not possible, however, because they only present whole-rock analyses. Other than the Aniakchak tephra, none of the tephra beds can be confidently correlated with others that have been described from western Alaska. The age of Tephra D overlaps with tephra beds of 'Lethe average' composition known from the Bristol Bay lowland, Alaska Peninsula and Cook Inlet area (Riehle *et al.*, 2008), but none of the late Pleistocene Lethe-like tephras analyzed previously have SiO_2 contents as low as Tephra D. Similarly, the age of one or more of the tephra beds described from the south-west Alaska Peninsula (Carson *et al.*, 2002) is permissive of a correlation, but the major-element geochemistries of the tephra beds in the Cold Bay area are dissimilar from the Ahklun Mountain deposits.

Conclusions

(i) Radiocarbon-dated sediment cores from six lakes and a soil pit in the Ahklun Mountains, south-western Alaska, were used to interpolate the ages of 26 visually detectable tephra beds. Of these, seven could be correlated between two or more sites on the basis of their ages. At least five other beds appeared to be present at only one site, based on their unique geochemistry or age, or both. Most of these unique tephra beds are known only from Lone Spruce Pond. Only two tephra beds were consistently found in all lakes, the Aniakchak tephra (3.7 ± 0.2 ka) and Tephra B (6.1 ± 0.3 ka).

(ii) Age uncertainties for individual tephra beds averaged ± 199 a, similar to the overall uncertainty of the age–depth models themselves. The $1\sigma_x$ age uncertainty for the seven tephra beds that were dated at more than one site averaged 115 a. In nearly all cases, the confidence intervals for the age–depth models overlapped with the mean age of the tephra, indicating that the confidence intervals output by the age–depth modeling routine *clam* (Blaauw, 2010) are reliable indicators of the reproducibility of the event ages.

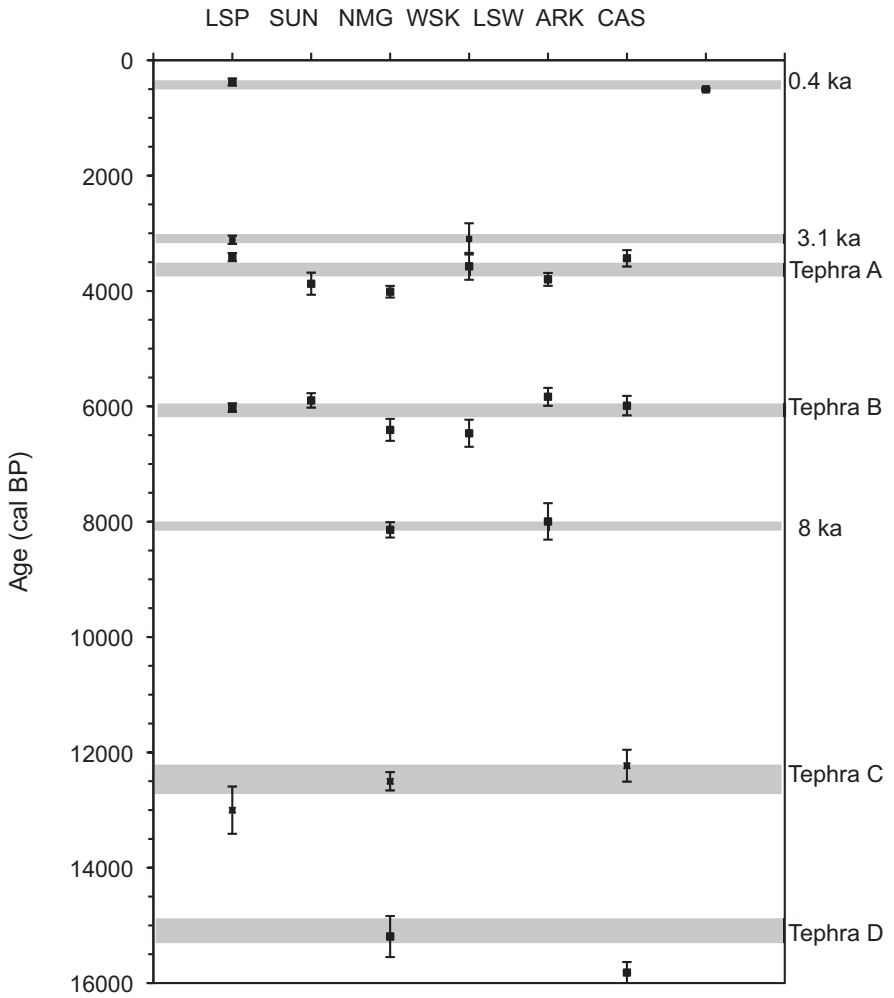

Figure 10. Summary figure showing the ages of the seven tephra beds that were found at more than one site. Error bars are $\pm 2\sigma$ confidence intervals derived from the *clam* age–depth modeling routine (Blaauw, 2010). Gray bands are the $\pm 1\sigma_x$ associated with the mean ages of each tephra bed as dated at multiple sites. Lakes are arranged from lowest to highest age-model uncertainty. LSP, Lone Spruce Pond; SUN, Sunday Pond; NMG, Nimgun Lake; WSK, Waskey Lake; LSW, Little Swift Lake; ARK, Arolik Lake; CAS, Cascade Lake soil pit. Data are listed in Table 5.

(iii) The major-element geochemistry of the tephra glass generally ranges from basaltic andesite to rhyolite, with some grains transitioning to trachyandesite and trachydacite. Most tephra beds have a unimodal composition. Others, including Tephra A (Aniakchak tephra), the thickest and most widespread in the region, exhibit a distinctly bimodal population, with a rhyolitic mode and an andesitic to basaltic–andesitic mode. The 3.1- and 0.4-ka tephra beds exhibit indistinguishable major- and trace-element compositions. These beds might indicate widespread reworking of Tephra A during times of landscape destabilization, or they are primary deposits with geochemical composition indistinguishable from Tephra A. The Lone Spruce Pond 5.8-ka tephra also has a bimodal major-element geochemistry that is indistinguishable from Tephra A, while its trace-element composition is distinct from Tephra A.

(iv) Excluding the Aniakchak tephra (Tephra A) and the beds with identical major-element geochemisty, we present eight new unique tephra beds: Tephra B, Tephra C, Tephra D, Tephra E, Lone Spruce Pond 4.7-ka tephra, Sunday Pond 5.3-ka tephra, Little Swift Lake 8-ka tephra and potentially the Sunday Lake (8 ka?) tephra. The tephra beds serve as isochrons for other undated sedimentary sequences in the region, although the presence of beds with nearly identical major-element compositions and different ages demonstrates that some age and stratigraphic control is needed to discern among tephra beds on the basis of their major-element geochemistry. Tephra A and Tephra B, and possibly the Lone Spruce Pond 5.8-ka tephra, were identified in a core from Cascade Lake. Tephra B, Tephra C and possibly the 8-ka tephra have now been located in sediment from Sunday Lake.

Supporting information

Additional supporting information can be found in the online version of this article:

Table S1. Major-element geochemistry of individual grains

Table S2. Summary of trace-element geochemistry of Aniakchak, 5.8-ka, 3.1-ka and 0.4-ka tephra beds.

Please note: This supporting information is supplied by the authors, and may be re-organized for online delivery, but is not copy-edited or typeset by Wiley-Blackwell. Technical support issues arising from supporting information (other than missing files) should be addressed to the authors.

Acknowledgements. Many colleagues and students during the past 15 years have helped to collect and analyze the cores from the eight lakes in this study, including R. S. Anderson, Y. Axford, J. Briner, T. Daigle, E. Dopfel, A. Feinberg, K. Kathan, B. Laabs, S. Lamoureux, L. Levy, H. Roop and (not least) A. Werner. Radiocarbon and plutonium isotope analyses were performed by T. Brown, M. Ketterer and J. Southon. The US Fish & Wildlife Service Dillingham Office provided logistical support for fieldwork. K. Wallace, Alaska Volcano Observatory, provided valuable input to this study. S. Matveev facilitated the electron microprobe analysis. J. Addison and D. Lowe provided helpful reviews of the manuscript. This research was funded by the National Science Foundation, most recently through award EAR-0823522 (DSK), and the Natural Sciences and Engineering Research Council of Canada (DGF).

Abbreviations. AMS, accelerator mass spectrometry; REE, rare earth elements.

References

Axford Y, Kaufman DS. 2004. Late glacial and Holocene glacier and vegetation fluctuations at Little Swift Lake, southwestern Alaska, U.S.A. *Arctic, Antarctic, and Alpine Research* **36**: 139–146.

Begét J, Mason O, Anderson P. 1992. Age, extent and climatic significance of the ca. 3400 BP Aniakchak tephra, western Alaska, USA. *The Holocene* **2**: 51–56.

Blaauw M. 2010. Methods and code for 'classical' age-modelling of radiocarbon sequences. *Quaternary Geochronology* **5**: 512–518.

Browne BL, Eichelberger JC, Neal CA, *et al*. 2004. The ~400 yr BP caldera-forming eruption of Half Cone Volcano, Aniakchak National Park, Alaska. General Assembly of the International Association of Volcanology and Chemistry of the Earth's Interior, 14–19 November 2004, Pucón, Chile (abstract). [Available at University of Alaska Fairbanks Library.]

Carson EC, Fournelle JH, Miller TP, *et al*. 2002. Holocene tephrochronology of the Cold Bay area, southwest Alaska Peninsula. *Quaternary Science Reviews* **21**: 2213–2228.

Denton JS, Pearce NJG. 2008. Comment on 'A synchronized dating of three Greenland ice cores through the Holocene' by B.M. Vinther *et al*.: no Minoan tephra in the 1642 B.C. layer of the GRIP ice core. *Journal of Geophysical Research* **113**: D04303.

Dreher ST, Eichelberger JC, Larsen JF. 2005. The petrology and geochemistry of the Aniakchak caldera-forming ignimbrite, Aleutian Arc, Alaska. *Journal of Petrology* **46**: 1747–1768.

de Fontaine CS, Kaufman DS, Anderson RS, *et al*. 2007. Late Quaternary distal tephra-fall deposits in lacustrine sediments, Kenai Peninsula, Alaska. *Quaternary Research* **68**: 64–78.

Feinberg AE. 2000. *Evidence of Holocene glacial activity from the Ahklun Mountains, southwestern Alaska*. BA thesis, Mt Holyoke College, South Hadley, MA.

Hu FS, Lee BY, Kaufman DS, *et al*. 2002. Response of tundra ecosystem in southwestern Alaska to Younger-Dryas climatic oscillation. *Global Change Biology* **8**: 1156–1163.

Jensen BJL, Froese DG, Preece SJ, *et al*. 2008. An extensive middle to late Pleistocene stratigraphic record from east-central Alaska. *Quaternary Science Reviews* **27**: 411–427.

Jochum KP, Stoll B, Herwig K, *et al*. 2006. MPI-DING reference glasses for in situ microanalysis: New reference values for element concentrations and isotope ratios. *Geochemistry, Geophysics, Geosystems* **7**: Q02008.

Kathan K. 2006. *Late Holocene climate fluctuations at Cascade lake, northeastern Ahklun Mountains, southwestern Alaska*. MS thesis, Northern Arizona University, Flagstaff, AZ.

Kaufman DS, Manley WF, Forman SL, *et al*. 2001. Paleoenvironment of the last interglacial-to-glacial transition, Togiak Bay, southwestern Alaska. *Quaternary Research* **55**: 190–202.

Kaufman DS, Hu FS, Briner JP, *et al*. 2003. A ~33,000 year record of environmental change from Arolik Lake, Ahklun Mountains, Alaska. *Paleolimnology* **30**: 343–362.

Ketterer ME, Hafer KJ, Jones VJ, *et al*. 2004. Rapid dating of recent sediments in Loch Ness: ICPMS measurements of global fallout plutonium. *Science of the Total Environment* **322**: 221–229.

Levy LB. 2002. *A record of late Holocene glacier fluctuations, Ahklun Mountains, southwestern Alaska*. MS thesis, Northern Arizona University, Flagstaff, AZ.

Levy LB, Kaufman DS, Werner A. 2004. Holocene glacier fluctuations, Waskey Lake, northeastern Ahklun Mountains, southwestern Alaska. *The Holocene* **14**: 185–193.

Lowe DJ. 2011. Tephrochronology and its application: a review. *Quaternary Geochronology* **6**: 107–153.

Manley WF, Kaufman DS, Briner JP. 2001. Late Quaternary glacial history of the southern Ahklun Mountains, southeast Beringia — Soil development, morphometric, and radiocarbon constraints. *Quaternary Science Reviews* **20**: 353–370.

Miller TP, Smith RL. 1987. Late Quaternary caldera-forming eruption in the eastern Aleutian arc, Alaska. *Geology* **15**: 434–438.

Neal CA, McGimsey RB, Miller TP, *et al*. 2001. Preliminary volcanice-hazard assessment for Aniakchak volcano, Alaska. *U.S. Geological Survey Open-File Report 00-519*.

Pearce NJG, Perkins WT, Westgate JA, *et al*. 1997. A compilation of new and published major and trace element data for NIST SRM 610 and NIST SRM 612 glass reference materials. *Geostandards Newsletter* **21**: 115–144.

Pearce NJG, Perkins WT, Westgate JA, *et al*. 2011. Trace element analysis by laser ablation ICP-MS: the quest for comprehensive chemical characterisation of single sub-10 um volcanic glass shards. *Quaternary International* **246**: in press.

Pearce NJG, Westgate JA, Preece SJ, *et al*. 2004. Identification of Aniakchak (Alaska) tephra in Greenland ice core challenges the 1645 BC date of Minoan eruption of Santorini. *Geochemistry, Geophysics, Geosystems* **5**: Q03005.

Pyne-O'Donnell S. 2011. The taphonomy of last glacial–interglacial transition (LGIT) distal volcanic ash in small Scottish lakes. *Boreas* **40**: 131–145.

R Development Core Team. 2010. *R: A language and environment for statistical computing*. R Foundation for Statistical Computing, Vienna.

Reimer PJ, Baillie MGL, Bard E, *et al*. 2009. IntCal09 and Marine09 radiocarbon age calibration curves, 0-50,000 years cal BP. *Radiocarbon* **51**: 1111–1150.

Riehle JR, Meyer CE, Ager TA, *et al*. 1987. The Aniakchak tephra deposit, a late Holocene marker horizon in western Alaska. *US Geological Survey Circular* **998**: 9–22.

Riehle JR, Ager TA, Reger RD, *et al*. 2008. Stratigraphic and compositional complexities of the late Quaternary Lethe tephra in south-central Alaska. *Quaternary International* **178**: 210–228.

Stuiver M, Reimer PJ. 1993. Extended ^{14}C database and revised CALIB 3.0 ^{14}C calibration program. *Radiocarbon* **35**: 215–230.

Sun S, McDonough WF. 1989. Chemical and isotopic systematics of oceanic basalts: implications for mantle compositions and processes. In Sanders AD, Norry MJ (Eds), *Magmatism in the Ocean Basins*. Geological Society Special Publication: 33–345.

Telford RJ, Heegaard E, Birks HJB. 2004. The intercept is a poor estimate of a calibrated radiocarbon age. *The Holocene* **14**: 296–298.